Available online at www.sciencedirect.com
ScienceDirect
Bioorganic & Medicinal Chemistry 16 (2008) 3759–3772
Bioorganic & Medicinal Chemistry

Selective plasma protein binding of antimalarial drugs to α_1-acid glycoprotein

Ferenc Zsila,* Júlia Visy, György Mády and Ilona Fitos

Department of Molecular Pharmacology, Institute of Biomolecular Chemistry, Chemical Research Center, Budapest, PO Box 17, H-1525, Hungary

Received 21 September 2007; revised 21 January 2008; accepted 30 January 2008
Available online 2 February 2008

Abstract—Human plasma protein binding of six antimalarial agents of quinoline and acridine types was investigated by using spectroscopic techniques, affinity chromatography, ultrafiltration and HPLC methods. Induced circular dichroism (ICD) spectra showed binding of amodiaquine (AMQ), primaquine (PRQ), tafenoquine (TFQ), and quinacrine (QR) to α_1-acid glycoprotein (AAG), the serum level of which greatly increases in *Plasmodium* infections. Association constant (K_a) values of about 10^5–10^6 M^{-1} could be determined. Analysis of the ICD and UV spectra of the drug–AAG complexes suggested the inclusion of the ligands into the central hydrophobic cavity of the protein. Using the purified forms of the two main genetic variants of AAG, ICD data indicated the selective binding of AMQ and PRQ to the 'F1/S', while QR to the 'A' variant. Results of fluorescence experiments supported the AAG binding of these drugs and provided further insights into the binding details of TFQ and QR. Fluorescence and CD displacement experiments showed the high-affinity AAG binding of mefloquine ($K_a \approx 10^6$ M^{-1}). For this drug, inverse binding stereoselectivities were found with the 'F1/S' and 'A' genetic variants of AAG. HSA association constants estimated from affinity chromatography results lag behind (10^3–10^5 M^{-1}) the similar values derived for AAG. In case of chloroquine, no significant binding interaction was found either with AAG or HSA. Pharmacological aspects of the results are discussed.

1. Introduction

Among the human plasma proteins albumin (HSA) and α_1-acid glycoprotein (AAG) give the largest contribution to serum protein binding of drugs. The normal plasma concentrations of HSA and AAG are 40 mg/mL; 600 μM and 0.5–1.4 mg/mL; 12–30 μM, respectively. HSA (585 residues, M_w = 66,500) appears to have high binding affinity for acidic and neutral compounds at two main binding sites located in subdomains IIA (site I) and IIIA (site II).[1] In contrast, basic drugs tend to bind preferably to the heavily glycosylated AAG (183 residues, M_w = 36,000–44,000).[2] The exact three-dimensional structure of AAG is still unknown. It belongs to the so called lipocalin protein family, characterized by a common tertiary structure with typical β-barrel motif, which functions as a hydrophobic pocket accomodating various ligands.[3] AAG exists in two main polymorphic forms called 'F1/S' (ORM1) and 'A' (ORM2) genetic variants, which show different drug binding properties.[4,5] The genetic variants are encoded by two different genes having 22/183 codon substitutions.[6] The biological function of this protein is not clear, although a number of in vitro and in vivo activities have been described. Beside the plasma transportation of a wide range of basic and neutral compounds, AAG has also been classified as a member of the immunocalin family, a lipocalin subfamily that modulates immune and inflammatory responses.[2,7]

Various disease states can significantly alter the concentrations of plasma proteins hereby modifying the free/bound fractions of pharmaceutical agents. It results in altered therapeutic effectiveness of highly protein-bound drugs. Similarly to other negative acute-phase proteins, synthesis of HSA is greatly depressed during acute-

Abbreviations: AAG, α_1-acid glycoprotein; AMQ, amodiaquine; CD, circular dichroism; CE, Cotton effect; CLQ, chloroquine; HSA, human serum albumin ICD, induced circular dichroism; L/P, ligand/protein molar ratio; MFQ, mefloquine; PRQ, primaquine; QR, quinacrine; TFQ, tafenoquine; UV/VIS, ultraviolet–visible.

Keywords: Acute-phase reaction; Antimalarial drugs; Fluorescence probes; Human serum α_1-acid glycoprotein; Human serum albumin; Induced circular dichroism; Malaria; Plasma protein binding; Genetic variants; Stereoselective binding.

* Corresponding author. Fax: +36 1 325 7750; e-mail: zsferi@chemres.hu

0968-0896/$ - see front matter © 2008 Elsevier Ltd. All rights reserved.
doi:10.1016/j.bmc.2008.01.053

phase reactions induced by stressful insults such as acute infections, trauma, cancer, and autoimmune diseases.[8] In contrast, serum concentration of the positive acute-phase reactant AAG increases 2- to 10-fold under the same conditions.[2,9]

Antimalarial agents are typical examples for drugs administered in acute-phase conditions.[10] They are in use primarily for treatment and prophylaxis of various forms of malaria but quinacrine (QR) and chloroquine (CLQ) also show therapeutic benefits in autoimmune diseases such as rheumatoid arthritis, lupus erythematosus, and sarcoidosis.[11,12] In acute *Plasmodium falciparum* malaria serum concentrations of AAG in non-immune patients increased twofold within 24 h compared to control subjects; while plasma level of HSA decreased by 30%.[13] Two- to threefold increase in serum AAG concentrations have been reported in arthritis and lupus erythematosus.[9] Protein-energy malnutrition is highly prevalent in developing countries where malaria is endemic. In undernourished subjects, serum albumin concentration falls while AAG was found above the normal level and caused a significant decrease in the free fraction of the test drug propranolol.[14] Negative correlation has been reported between the plasma level of AAG and the free fraction of quinine in children with falciparum malaria, too.[15]

Numerous antimalarial compounds used in the clinical practice including 4-aminoquinolines such as amodiaquine (AMQ) and CLQ, the 8-aminoquinoline primaquine (PRQ) and tafenoquine (TFQ), quinoline methanols (MFQ, quinine, quinidine), and acridine derivatives (QR) possess a heteroaromatic moiety and an aliphatic or alicyclic side chain containing an amino group protonated at physiological pH (Fig. 1). Based on these structural properties it can be expected that these drugs may preferentially bind to AAG. Except for quinine and quinidine,[2,16] however, details of their binding interactions with AAG and HSA have not been determined yet.

Recently, circular dichroism (CD) and electronic absorption spectroscopy have successfully been used to demonstrate the AAG binding of the antimalarial

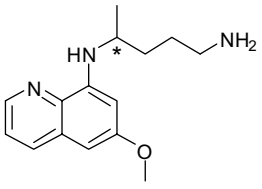

Primaquine (PRQ)
N-(6-methoxyquinolin-8-yl)
pentane-1,4-diamine

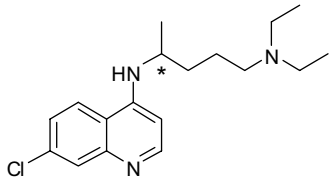

Chloroquine (CLQ)
N'-(7-chloroquinolin-4-yl)-
N,N- diethyl-pentane-1,4-diamine

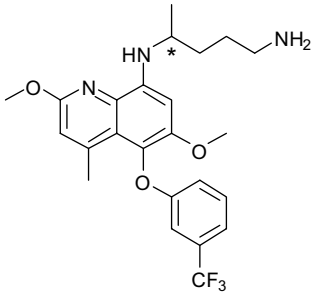

Tafenoquine (TFQ)
N-[2,6-dimethoxy-4-methyl-5-
[3-(trifluoromethyl)phenoxy]quinolin-8-yl]
diamine

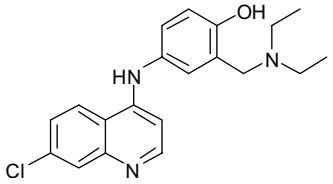

Amodiaquine (AMQ)
4-[(7-chloroquinolin-4-yl)amino]
-2-(diethylaminomethyl)phenol

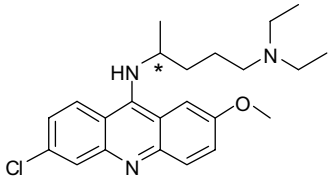

Quinacrine (QR)
N'-(6-chloro-2-methoxy-acridin-9-yl)
-N,N-diethyl-pentane-1,4-diamine

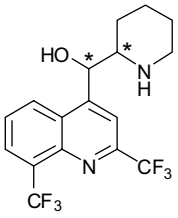

Mefloquine (MFQ)
[2,8-bis(trifluoromethyl)quinolin-4-yl]
-(2-piperidyl)methanol

Figure 1. Chemical structures of antimalarial drugs studied in this work. Asterisks denote asymmetric centers.

agents PRQ and MFQ.[17] From the analysis of the extrinsic CD signals induced by the protein environment, inclusion of the drug molecules into the central hydrophobic cavity of AAG near to the Trp25 residue was concluded. Induced CD (ICD) spectra provided evidence for the high-affinity binding of QR to chicken AAG, as well.[18] Human AAG association of QR-related acridine compounds and the antimalarial xanthene dye rhodamine B was also demonstrated by employing CD spectroscopy.[5,17]

In the current study CD, UV/VIS absorption and fluorescence spectroscopic techniques have been used to investigate the binding of six antimalarial compounds (Fig. 1) to AAG and HSA, in order to obtain some information for their pharmacokinetic, pharmacodynamic and toxicological profiles. Some experiments were performed also with the separated genetic variants of AAG. HSA binding affinities were evaluated by affinity chromatography. Stereoselective binding of MFQ to AAG was investigated by combined ultrafiltration and chiral HPLC techniques.

2. Results

2.1. Circular dichroism and UV/VIS spectroscopic studies of AAG binding of PRQ, TFQ, AMQ, and QR

Binding interaction of small molecules with the protein host often induces changes in the optical spectra of the guest represented by a red/blue shift and/or intensity increase/decrease of the absorption bands reflecting the environmental change (from bulk solvent to the binding site) of the guest chromophore. In addition, such complexes may exhibit extrinsic CD activity due to the chiral perturbation of the electronic transitions of the ligands by the asymmetric protein surroundings.[18,19] By this way, CD spectroscopy provides a powerful method to detect the formation of drug–protein complexes and for characterization of ligand binding modes.

The CD curve of AAG displays multiple, weak positive signals between 250 and 310 nm (data not shown). Under simulative physiological conditions (37 °C, pH 7.4 Ringer buffer) four of the studied antimalarial drugs, AMQ, PRQ, QR, and TFQ showed definite extrinsic CD bands upon their addition into AAG solution. These compounds are either achiral (AMQ) or racemic mixtures (PRQ, QR, TFQ) so they do not have intrinsic CD activities in protein free solutions. Thus, appearance of difference CD bands, obtained by subtracting the CD contribution of AAG from that of the drug-protein mixtures, clearly indicates the binding of these drugs to the asymmetric protein binding site.

The shape of the single positive Cotton effect (CE) of protein-bound PRQ strongly resembles its UV absorption band which is red shifted in relation to the absorption peak of the free drug (Fig. 2).

A similar, but smaller shift was observed in the UV spectrum of AAG-bound TFQ which showed two asymmetric CEs in the UV absorption region, a stronger long-wavelength positive and a weaker short-wavelength neg-

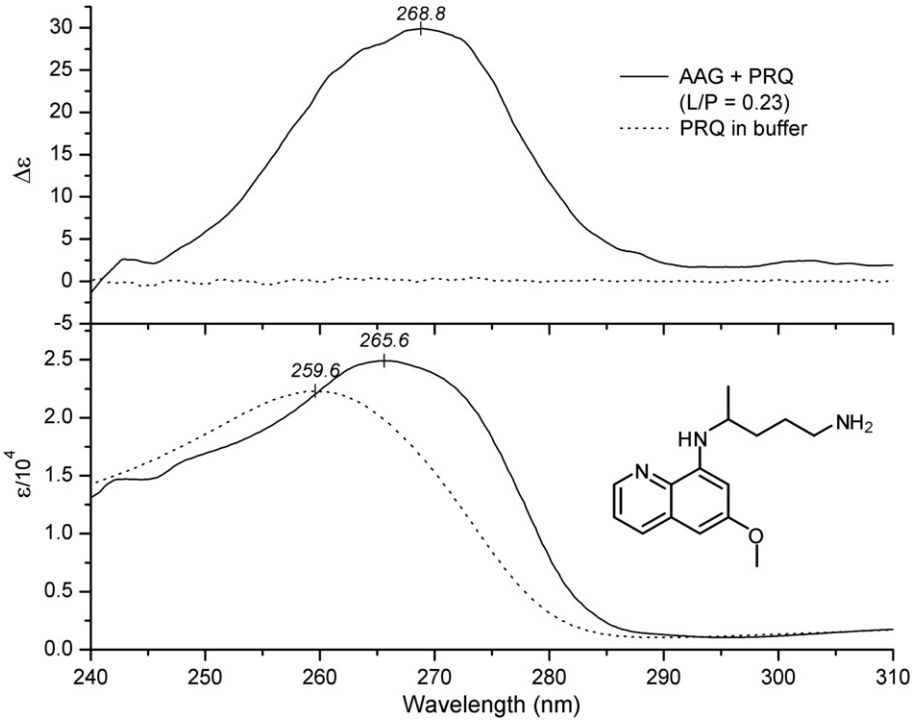

Figure 2. Difference CD and UV absorption spectra of (±)-PRQ diphosphate in the presence of 40 μM AAG and in protein-free Ringer buffer solution at 37 °C. [PRQ] = 9 μM.

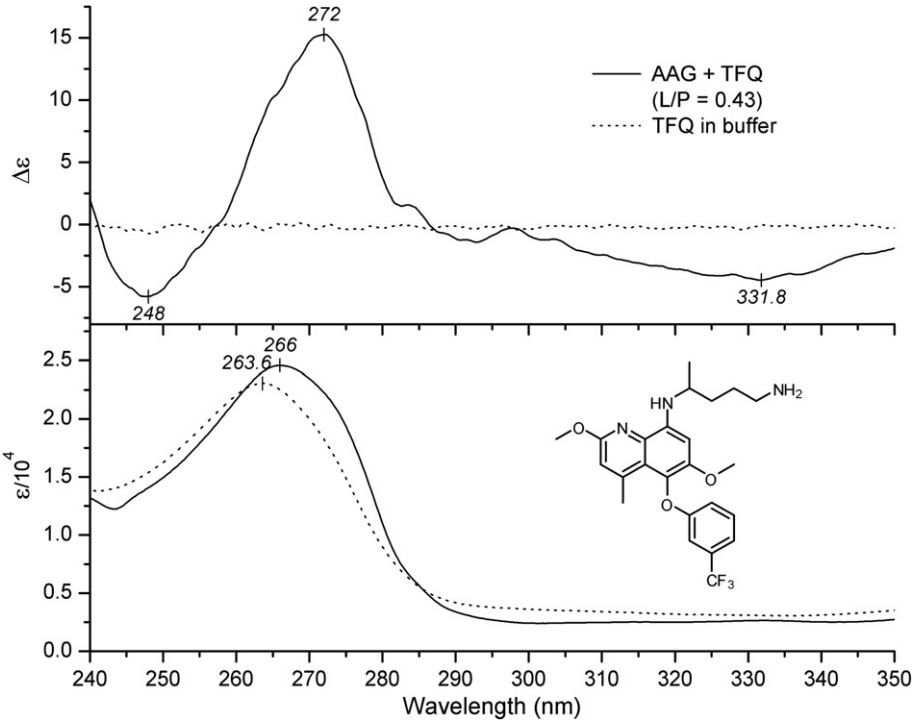

Figure 3. Difference CD and UV absorption spectra of (±)-TFQ in the presence of 28 μM AAG and in protein-free Ringer buffer solution at 37 °C. [TFQ] = 12 μM.

ative one at 272 and 248 nm (Fig. 3). An additional broad, negative CD band was also induced between 300 and 350 nm where TFQ displays no definite absorption peaks.

Binding of AMQ to AAG resulted in two, a stronger negative and a very weak positive ICD peaks above 300 nm, centered over the short- and long-wavelength tails of the absorption band (Fig. 4). Only a slight red-

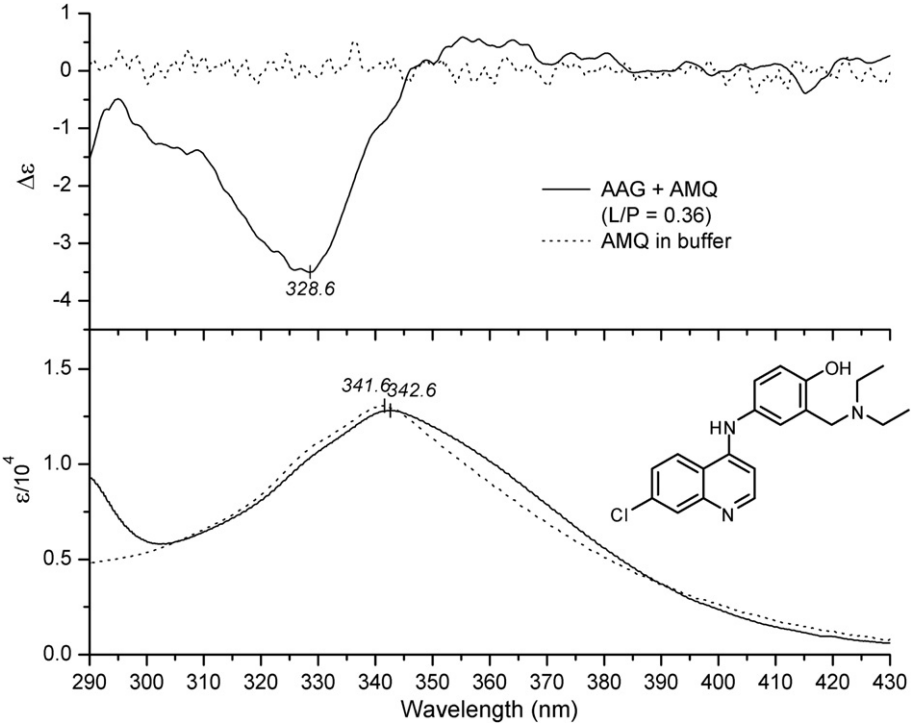

Figure 4. Difference CD and UV absorption spectra of AMQ hydrochloride in the presence of 47 μM AAG and in protein-free Ringer buffer solution at 37 °C. [AMQ] = 17 μM.

shift of the UV λ_{max} of AMQ was seen in the AAG-bound state.

Difference CD curve of QR–AAG mixture displayed low-intensity positive ICD bands both in the visible and in the UV absorption regions (Fig. 5A and B). Spectral positions of the UV and VIS CEs correspond to the relevant absorption bands of the drug. Next to the short-wavelength ICD peak, a much weaker negative dichroic band also appeared around 294 nm (Fig. 5B). In relation to the spectrum recorded in buffer solution, the UV and VIS absorption bands of AAG-bound QR were shifted in opposite directions: while the UV peak exhibited a bathochromic shift, λ_{max} of the visible band was

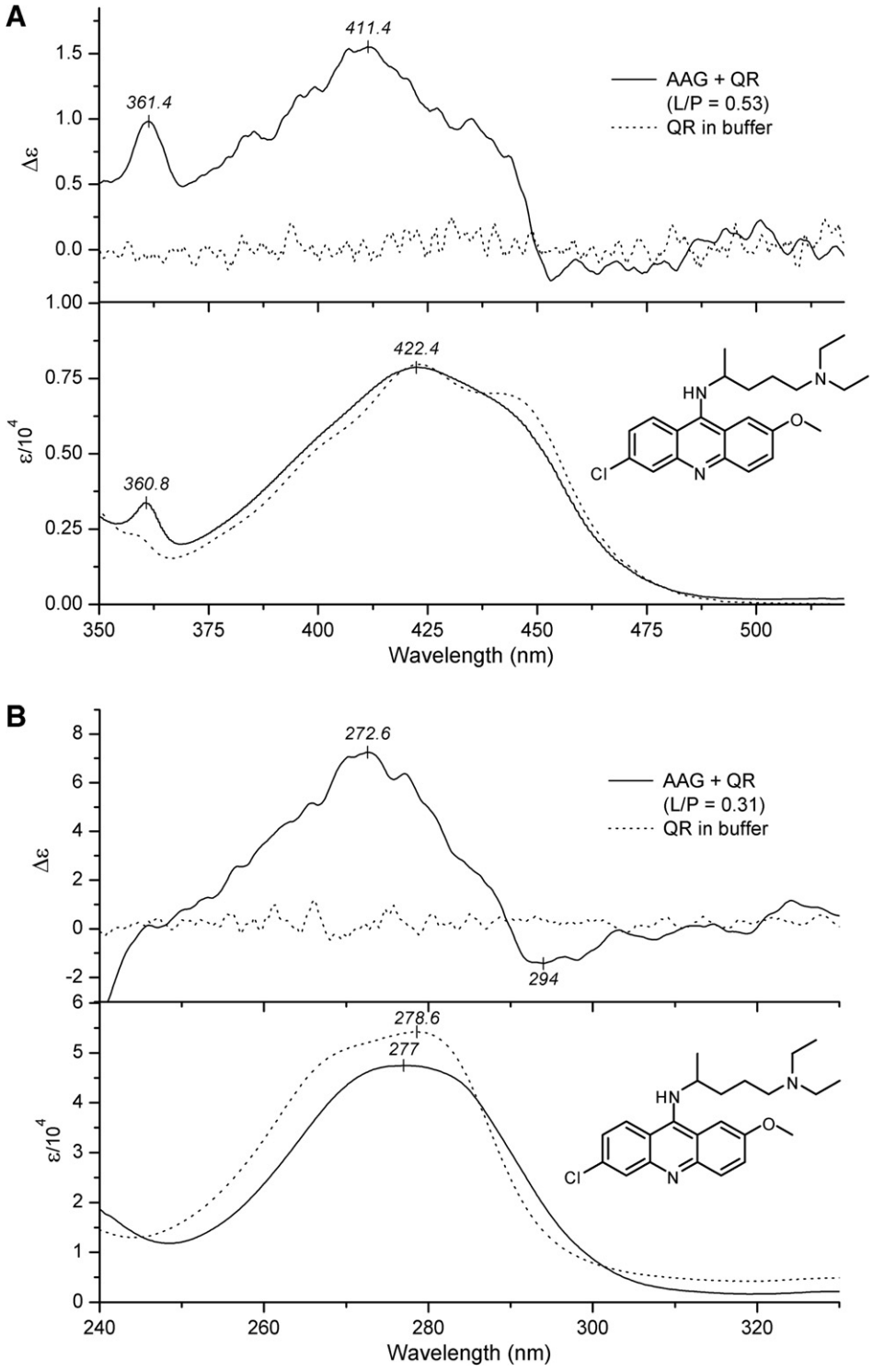

Figure 5. (A) Difference CD and VIS absorption spectra of (±)-QR dihydrochloride in the presence of 69 μM AAG and in protein-free Ringer buffer solution at 37 °C. [QR] = 37 μM. (B) Difference CD and UV absorption spectra of (±)-QR dihydrochloride in the presence of 22 μM AAG and in protein-free Ringer buffer solution at 37 °C. [QR] = 8 μM.

moved to slightly shorter wavelengths. It could also be observed that in contrast to the protein-free condition, vibrational fine structures of both the UV and VIS absorption bands were suppressed (Fig. 5A and B).

Upon titration of a fixed amount of AAG with increments of the four antimalarial drugs, the ICD values at constant wavelength indicate the actual bound ligand concentrations. The values of the association binding constants (K_a) and the number of binding sites per AAG molecule (n) were calculated from the ICD data (Table 1) by applying nonlinear regression analysis. In case of TFQ the ICD titration experiment was repeated at 23 °C, because large difference was obtained for the K_a values by the ICD and fluorescence approaches (cf. Tables 1 and 2). The binding constant obtained at 23 °C was much higher (1.1×10^6 M^{-1}), being in agreement with the value estimated from the fluorescence data (1.8×10^6 M^{-1}). From this unusually large temperature dependence, according to the van't Hoff equation thermodynamic parameters of $\Delta G = -34$ kJ mol^{-1}, $\Delta H = -65$ kJ mol^{-1} and $\Delta S = -104$ J mol^{-1} K^{-1} can be calculated.

Since commercial AAG samples consist of the 'A' and 'F1/S' genetic variants approximately in 30/70 ratio,[4] some $n < 1$ values (Table 1) may reflect selective drug binding on the genetic variants (Table 1). The $n = 0.3$ value yielded from the analysis of ICD data of QR-native AAG complex suggests selective association of the drug to the 'A' variant. Therefore, 'A' variant solution was also titrated with QR recording CD and UV spectra below 335 nm. In relation to the curves found with the native protein (Fig. 5B), qualitatively the same but twice intense CE pair was obtained (Supplementary Fig. 1) supporting the 'A' variant binding specificity of QR. The larger bathochromic shift of the UV band lends further evidence to the existence of a high-affinity QR binding site on the 'A' variant. Accordingly, no ICD signal was observed upon addition of QR to the 'F1/S' variant solution (data not shown). Nevertheless, comparison of the UV spectra of the drug taken in buffer solution and in the presence of the 'F1/S' variant proves that QR–'F1/S' binding interaction also does occur, since the intensity ratio of the unresolved sub-bands of the UV peak is just the opposite, and a small, but definite bathochromic shift can be observed in the protein solution (Supplementary Fig. 2).

Evaluation of the ICD data of AMQ–AAG and PRQ–AAG interactions resulted in n values of 0.6 and 0.7 suggesting the 'F1/S' variant binding preference of these drugs. CD titration measurements were performed under the same conditions by using 'F1/S' protein sample. The ICD curves of PRQ–'F1/S' and AMQ–'F1/S' mixtures were similar to those obtained with the native protein (data not shown). The stoichiometry values confirmed the selective binding of these drugs on the 'F1/S' variant (Table 1).

The n value of about one derived for TFQ suggests that this drug does not discriminate between the genetic variants of AAG.

Table 1. In vitro binding parameters of antimalarial drugs on AAG estimated from ICD spectroscopic data at 37 °C

	K_a (M^{-1})	n
Amodiaquine diHCl (λ = 328 nm)	Native 4.8 (±0.6) × 10^4	0.6
	'F1/S' 5.8 (±0.4) × 10^4	0.9
Primaquine diphosphate (λ = 269 nm)	Native 4.1 (±1.0) × 10^5	0.7
	'F1/S' 8.0 (±1.8) × 10^5	0.9
Quinacrine diHCl (λ = 271.6 nm)	Native 2.3 (±0.5) × 10^5	0.3
	'A' 3.7 (±0.8) × 10^5	0.8
Tafenoquine (λ = 272 nm)	Native 3.3 (±0.7) × 10^5	0.9
	*1.1 (±0.3) × 10^6	*1.0

Binding constant value of TFQ denoted by asterisk was calculated from ICD spectra measured at 23 °C.

Table 2. Binding constants of antimalarial and reference drugs for the binding on commercial AAG evaluated from quinaldine red displacement at room temperature

Drug	K_a (M^{-1})
CLQ	0.3 × 10^5
AMQ	1.1 × 10^5
PRQ	4.2 × 10^5
MFQ	8.7 × 10^5
TFQ	1.8 × 10^6
(±)-Propranolol	2.5 × 10^5
	[a]1.5 × 10^5
Chlorpromazine	8.4 × 10^5
	[a]9.6 × 10^5
Mifepristone	1 × 10^7
	[b]4 × 10^6

[a] Ref. 4.
[b] Ref. 25.

2.2. CD and UV/VIS spectroscopic investigations of CLQ–AAG interaction

Unlike PRQ (8-aminoquinoline), in AAG solution the 4-aminoquinoline drug CLQ did not show any ICD signal. Accordingly, the difference UV spectrum of CLQ obtained in the presence of AAG was practically identical to that recorded in buffer (not shown).

2.3. Demonstration of MFQ–AAG interaction by CD displacement experiments

The principal π–π* transition of the quinoline ring of MFQ is located below 230 nm (in EtOH, ε_{max} is 44,000 at 222.5 nm) where the strong intrinsic CD activity and light absorption of AAG prevent measuring reliable ICD data. Furthermore, no ICD signal was found in the low-intensity (ε_{max} is 5800 at 282.5 nm) UV absorption region of MFQ between 250 and 330 nm (not shown). Thus, AAG binding ability of MFQ was tested indirectly by using the CD displacement method.[20,49] Consecutive addition of MFQ to a drug–AAG complex showing ICD activity above 240 nm may result in the decrease or complete extinction of the ICD signal due to competition for the same drug binding area. AAG complexes of AMQ, PRQ, and TFQ were selected to study the effect of MFQ on their extrinsic CEs (Fig. 6). Amplitude of the ICD peak of AMQ de-

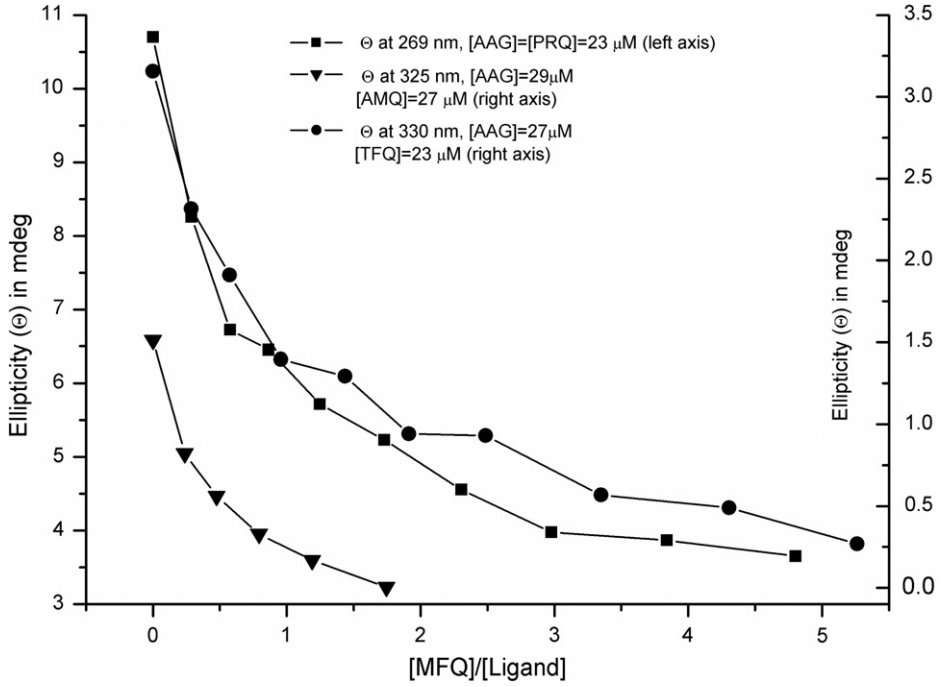

Figure 6. Results of CD displacement experiments performed with (±)-MFQ on drug–AAG complexes in Ringer buffer solution at 37 °C. MFQ was added as μl aliquots of ethanolic stock solution.

creased gradually upon addition of MFQ and reduced to zero between 1.7 and 2.4 molar ratio of [MFQ]/[AMQ]. In case of PRQ, however, the signal decreased quickly by 37%, but significant residual ICD activity was measured even at MFQ concentrations far higher than that of the AAG. The shape of the displacement curve of TFQ–AAG complex was similar to that obtained with PRQ but the residual ICD is less pronounced.

2.4. CD and UV/VIS spectroscopic study of HSA binding of antimalarial drugs

Interaction of AMQ with HSA induced a CD band pair in the near-UV region where the drug chromophore shows light absorption (Supplementary Fig. 3). Shape and spectral position of these CEs resemble those measured in the presence of AAG (Fig. 4) but they are more symmetric and their magnitudes are nearly equal. Absorption maximum of the albumin-bound AMQ is at slightly shorter wavelength compared either to the AMQ–AAG complex (Fig. 4) or to the protein-free spectra. Analysis of ICD values obtained at different [drug]/[HSA] molar ratios indicated weak binding ($K_a = 0.62 \times 10^4\ M^{-1}$) and $n = 1.1$ for the number of binding sites.

Difference CD curves of the TFQ–HSA mixture displayed less intense but analogous CEs as found with AAG (Supplementary Fig. 4). The UV band of TFQ, however, exhibited a larger red shift in the presence of albumin (cf. Fig. 3). Analysis of CD titration data indicated low-affinity ($K_a = 2.4 \times 10^4\ M^{-1}$) HSA binding for TFQ in 1:1 stoichiometry. Titration experiment performed at 23 °C also showed low intensity ICD values of irregular pattern.

Over the range of 240–500 nm, difference UV/VIS spectra of PRQ, QR, and CLQ added to HSA solution did not differ from those measured in buffer, and ICD activities could not be detected, either.

2.5. Evaluation of AAG binding affinities from quinaldine red displacement by fluorescence method

Quinaldine red is a specific fluorescent probe of AAG.[21–23] It is highly fluorescent in protein-bound state, the fluorescence of the free dye is negligible. Quenching of fluorescence of bound label by drugs is supposed to be of static nature, thus it reflects the decrease of bound label concentration. It is to be noted that fluorescence of bound quinaldine red in native AAG solution refers mostly to the 'F1/S' genetic variant.[23] The effect of five antimalarial agents and three reference drugs on the fluorescence of quinaldine red bound to AAG can be seen in Figure 7. The corresponding quenching constants (K_{SV}) according to the Stern-Volmer equation ($F_0/F = 1 + K_{SV}$ [quencher])[24] are given in Table 2.[4,25] The quenching constants are considered to be identical with the binding constants (K_a) of the displacers. It can be observed that the binding of CLQ is weak, AMQ is moderate, while PRQ, MFQ, and especially TFQ have high affinities for AAG. QR could not be investigated by this method because of its own fluorescence.

2.6. Study of TFQ and QR binding to AAG and HSA by fluorescence detection

TFQ was found to exhibit remarkably enhanced fluorescence emission in the presence of both AAG and HSA (Fig. 8a). Though the UV maximum of TFQ is at 264 nm (Fig. 3), the emission maxima wavelengths were

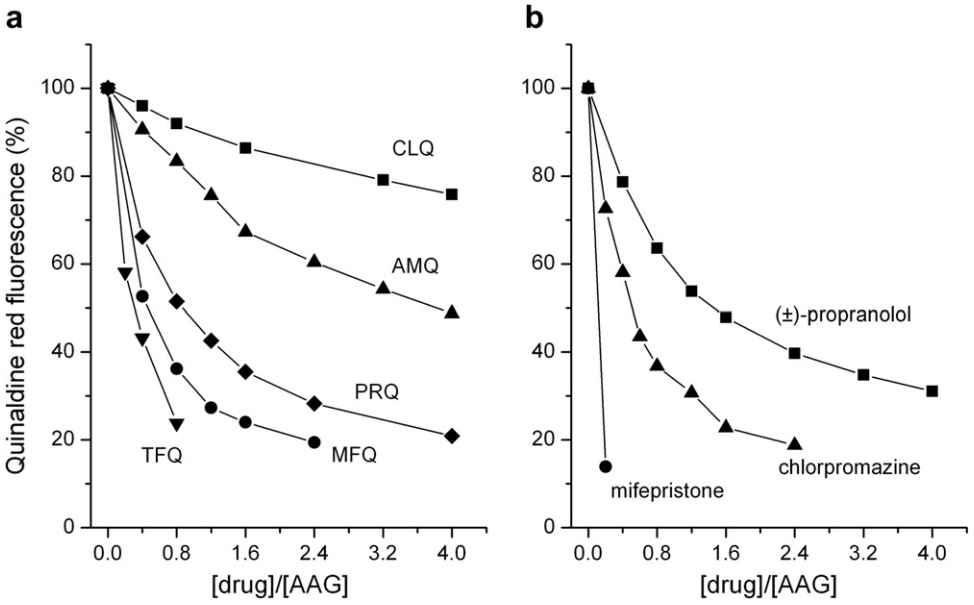

Figure 7. Quenching of 2 μM quinaldine red fluorescence in 2.5 μM AAG solution by antimalarial agents (a) and by reference drugs (b). Excitation and emission wavelengths were 495 and 576 nm, respectively.

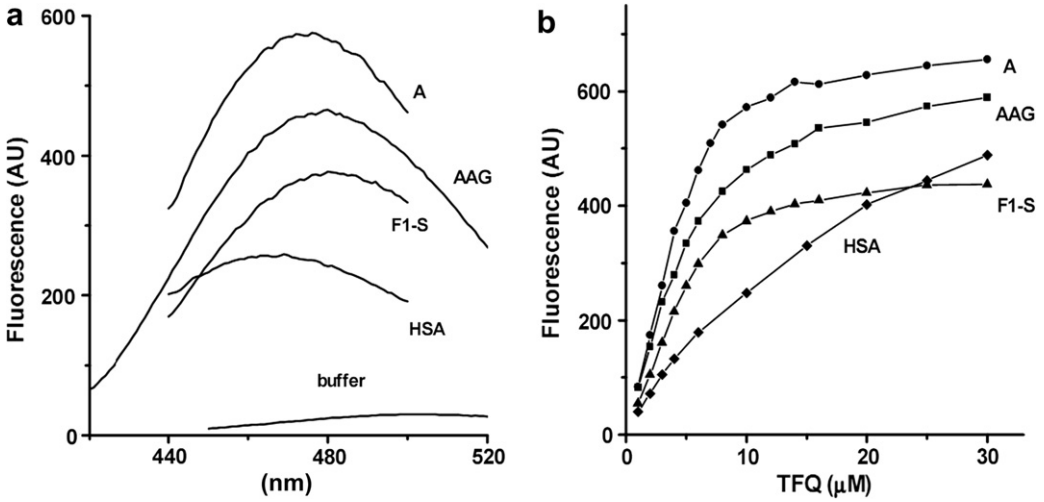

Figure 8. Fluorescence of (±)-TFQ in the presence of serum proteins (room temperature). (a) Fluorescence emission spectra of 10 μM TFQ in buffer as well as in different 10 μM protein solutions (commercial AAG, its 'F1/S' and 'A' genetic variants or HSA). Excitation was made at 300 nm; (b) Titration of 10 μM protein solutions by TFQ. Fluorescence intensities were read at the corresponding emission peak maxima.

as high as 505 nm in buffer, while 480 and 460 nm with AAG and HSA, respectively. Specific fluorescence values of fully bound TFQ were determined by mixing excess amount of protein crystals into the ligand solution or using data obtained at low L/P ratios. Excitation was made at 300 nm to avoid the disturbance of the scattered light. The fluorescence of TFQ with the AAG genetic variants was different. The complexes with the 'F1/S' and 'A' variants could be detected at 482 and 475 nm, respectively, and the specific fluorescence of the 'A' complex was about 1.6 times more intense compared to the 'F1/S' variant. Scatchard plots calculated from the titration curves (Fig. 8b) of different protein solutions resulted in nK_a values of about 1.6×10^6 and $3 \times 10^5\ M^{-1}$ for the binding of TFQ to AAG and HSA, respectively. The plots indicated the occurence of low-affinity secondary binding processes, too.

Since the UV band of QR suggested its association with the 'F1/S' variant too (Supplementary Fig. 2), fluorescence emission spectra of QR were recorded in buffer solution as well as in the presence of commercial AAG and its genetic variants. By the addition of QR into the protein solutions positions of the emission maxima displayed definite blue shifts and the quantum yields were enhanced (Fig. 9). Compared to the emission curve measured in Ringer buffer, the largest change was observed with the 'A' variant but significant blue shift and fluorescence intensity enhancement were also obtained with the 'F1/S' form.

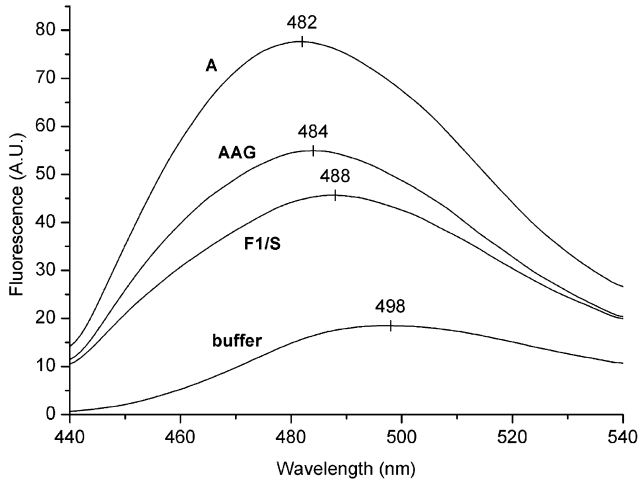

Figure 9. Fluorescence emission spectra of 1 μM (±)-QR dihydrochloride in buffer as well as in 10 μM AAG solutions (commercial AAG, its 'F1/S' and 'A' genetic variants). Excitation was made at 420 nm (room temperature).

2.7. HSA binding study by affinity chromatography

Binding affinity of the antimalarial drugs to HSA was evaluated from their retentions on a HSA-Sepharose column. Elution volumes are characteristic of the binding affinity (nK_a).[48] Oxazepam acetate and lorazepam acetate enantiomers, as well as diazepam, were used as reference compounds. Results in Table 3 indicate weak albumin binding for CLQ, PRQ, QR, and AMQ, while stronger binding for MFQ and especially for TFQ.

2.8. Study on the location of binding sites of MFQ and TFQ on HSA

Dansylsarcosine and dansylamide are specific fluorescence labels of the two main binding sites of HSA.[26] The effect of MFQ (1–20 μM) was investigated on the fluorescence of the labels (4 μM) in HSA (10 μM) solutions. Excitation and emission wavelengths were 350 and 480 nm, respectively. No fluorescence quenching could be detected. TFQ could not be investigated by this method because of its own fluorescence, so its binding site was tested in the inversed experimental setup. Fluorescence change of TFQ (10 μM) bound to HSA (15 μM) was studied in the presence of flurbiprofen and phenylbutazone, which are characteristic high-affinity ligands of the two major drug-binding sites of HSA.[26] No quenching could be detected. Thus, the binding of MFQ and TFQ probably occurs somewhere else on the protein.

Table 3. Elution volumes (V_e) and corresponding binding parameters (nK_a) obtained on a HSA-Sepharose column (eluent: Ringer buffer, pH 7.4, room temperature)

Sample	V_e (mL)	nK_a (M^{-1})	Reference
Solvent	6.5		
(*R*)-Oxazepam acetate	14	1×10^4	48
(*S*)-Oxazepam acetate	39	8×10^4	48
(*R*)-Lorazepam acetate	18	2×10^4	48
(*S*)-Lorazepam acetate	26.5	4×10^4	48
Diazepam	80	1.8×10^5	48
PRQ	9.5	$\approx 7 \times 10^3$	Estimated
CLQ	7.5	$\approx 2 \times 10^3$	Estimated
QR	9.5	$\approx 7 \times 10^3$	Estimated
AMQ	16	$\approx 2 \times 10^4$	Estimated
MFQ	39	$\approx 8 \times 10^4$	Estimated
TFQ	180	$\approx 3 \times 10^5$	Estimated

2.9. Stereoselective binding of MFQ to AAG and HSA

Stereoselective protein binding of *erythro*-MFQ was investigated by analyzing the enantiomer composition in the ultrafiltrates of solutions containing the racemic drug and the protein. In the experiment performed with 60 μM HSA and 10 μM MFQ no significant stereoselectivity was detected (not shown). The binding of MFQ to AAG, however, was found to be stereoselective. Chiral

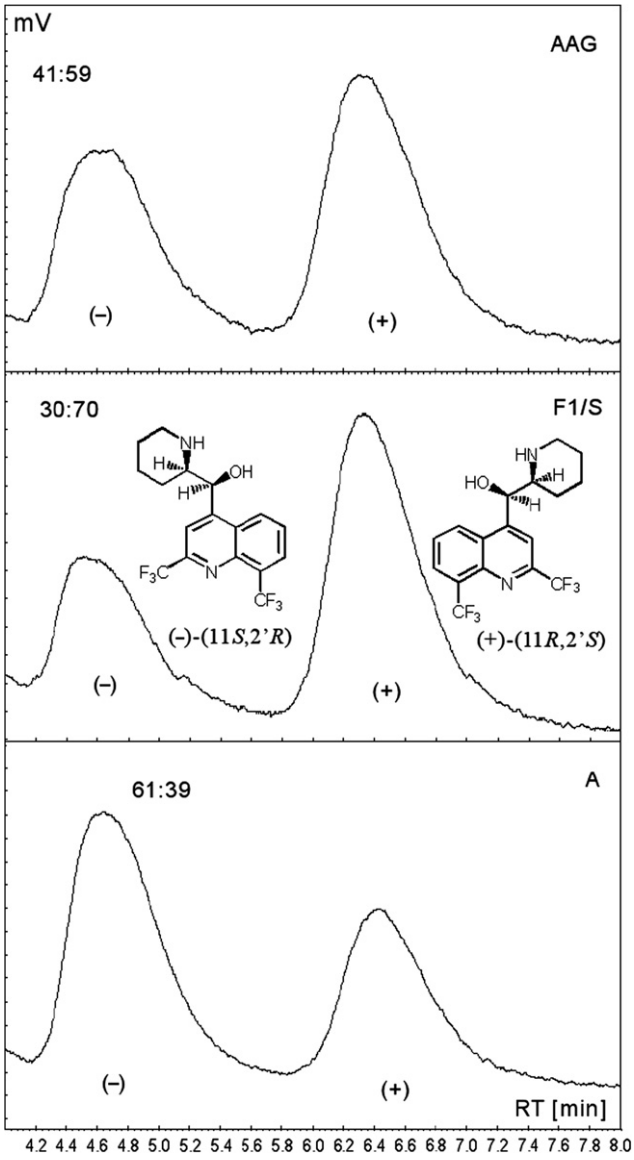

Figure 10. Enantiomeric composition of *erythro*-MFQ in the ultrafiltrates of solutions containing 4 μM racemic drug and 25 μM AAG or its 'F1/S' and 'A' genetic variants. HPLC analysis was made on chiral-AGP column.

HPLC analysis of the ultrafiltrates of solutions containing 4 μM racemic drug and 25 μM AAG showed enantiomeric ratio of (−)/(+):41/59 for the free drug, indicating the preferred binding of the (−)-enantiomer (Fig. 10). Similar experiments performed with the genetic variants of AAG revealed that the favored binding of the (−)-enantiomer occurs on the 'F1/S' variant. On the 'A' variant, which takes up about 30% of native AAG, the stereoselectivity is reversed, the binding of the (+)-enantiomer is stronger. From the enantiomeric compositions, stereoselectivity values of $K_a(-)/K_a(+) \approx 2.4$ and $K_a(+)/K_a(-) \approx 1.7$ could be evaluated[27] for the MFQ binding on the 'F1/S' and 'A' variants, respectively.

3. Discussion

The spectroscopic data presented above suggest that AAG is an important contributor in the plasma distribution of the antimalarial drugs studied here (except for CLQ). AAG binding of PRQ, TFQ, QR, and AMQ generated extrinsic CD bands in the UV absorption region of the ligands. MFQ binding to AAG could be revealed by indirect methods. HSA binding tests showed considerable binding only in cases of MFQ and TFQ (Table 3).

ICD activity of PRQ can be accounted for the non-degenerate exciton interaction between the π–π^* transitions of the quinoline moiety and of the Trp25 side chain near to the protein-bound drug.[17] Accordingly, the principal binding site of PRQ is inside the central hydrophobic cavity of the β-barrel fold of AAG where the Trp25 residue is located.[28] The large red-shift in the UV spectrum of PRQ (Fig. 2) indicates the inclusion of the quinoline chromophore into a strongly hydrophobic protein environment. ICD spectra of PRQ–AAG interaction could be referred to the 'F1/S' variant selective binding of the drug (Table 1). Fluorescence studies using the strongly fluorescent AAG marker quinaldine red showed that PRQ effectively displaces the dye from its protein binding site (Fig. 7). Since quinaldine red is bound inside the hydrophobic matrix of AAG, this finding further supports the cavity binding concept of PRQ. The affinity constant value of $4 \times 10^5\ M^{-1}$ PRQ estimated to PRQ from fluorescence displacement experiments (Table 2) is in good agreement with the value derived from the ICD data (Table 1). Notably, the binding affinity of PRQ to HSA was found to be about 60 times weaker (Table 3).

According to the ICD data, the PRQ derivative TFQ carrying a bulky phenoxy substituent has similar AAG binding affinity but do not discriminate between the genetic variants (Table 1). The spectral features of the principal extrinsic CEs of TFQ and PRQ as well as the bathochromic shift of their UV bands are highly similar to each other suggesting the binding of both drugs inside the β-barrel cavity of AAG. The same conclusion can be drawn from the quinaldine red displacement results (Fig. 7). The thermodynamic parameters revealed that the binding of TFQ to AAG is mainly enthalpy-driven. Negative enthalpy and entropy changes are usually characteristic of protein–ligand interactions, where van der Waals interactions and hydrogen bonds play major role.[29] The K_a value estimated from the fluorescence data ($3 \times 10^5\ M^{-1}$) showed much stronger HSA binding of TFQ in relation to the association constant calculated from the ICD spectra ($2.4 \times 10^4\ M^{-1}$). Distinctly from the case of AAG, this difference cannot be accounted for the temperature dependence. In addition, the irregularities of the ICD titration curves suggest some non-homogenous binding environments of TFQ on HSA. Thus, it can be assumed the ICD activity detected during TFQ–HSA interaction may indicate a secondary binding process. Fluorescence displacement tests showed that the binding of TFQ occurs neither on site I or site II of HSA. The larger red shift of the UV band of TFQ induced by the HSA binding (Supplementary Fig. 4) compared to that measured with AAG (Fig. 3) suggests the greater hydrophobicity of the primary drug-binding environment on albumin. The blue shifts of the fluorescence emission maxima of HSA- and AAG-bound TFQ are in accordance with this (Fig. 8a). Increase of the quantum yield and the shift of the emission maximum upon mixing drugs and proteins are the well-known indicators of the drug binding to the apolar protein matrix. Using the same ligand (TFQ) with different proteins (AAG and HSA), the extent of the blue shift correlates with the relative hydrophobicity of the binding sites.[30] Accordingly, chemical nature of the TFQ binding sites on the AAG variants is also different indicated by the unequal intensities and wavelength maxima of the emission spectra (Fig. 8a) showing the greater hydrophobicity of the 'A' variant site. In summary, high-affinity AAG and HSA binding should result in very extensive plasma protein binding of TFQ. Due to the large serum level difference the contribution of HSA must be dominant in the plasma protein binding of TFQ.

CD and UV spectra showed no sign of binding interaction either between CLQ and AAG or CLQ and HSA. Similarly, CLQ was practically ineffective in displacing quinaldine red from AAG (Fig. 7) and HSA affinity chromatography results indicated its weak albumin association (Table 3). All of these findings are in accordance with the low plasma protein binding of CLQ reported earlier.[31]

In case of AMQ which differs from CLQ in the side chain, some ICD activities were found with both proteins. In agreement with the quinaldine red displacement and HSA-chromatographic results, the evaluated binding constants indicated moderate binding, favoring the 'F1/S' variant of AAG (Table 1).

QR displayed ICD bands in the presence of AAG indicating formation of drug–protein complexes (Fig. 5, Supplementary Fig. 1), which could be referred to the 'A' genetic variant. Aromatic moieties of AAG ligands contribute to the protein binding via hydrophobic interactions (π–π stacking, van der Waals forces). Compared to the structurally similar but weak AAG ligand CLQ, extension of the aromatic moiety in QR seem to be important in its much stronger AAG binding. In contrast to the acridine dyes which provoke intense exciton couplet upon binding

to the 'A' variant in a dimeric form,[5] the stoichiometry values indicate the protein association of a single QR molecule (Table 1). The protein binding environment induces CD activity in the electronic transitions of QR by the analogous mechanism as in PRQ; that is, via non-degenerate exciton coupling between the π–π^* transitions of the acridine ring and an adjacent tryptophan residue.[17] Since racemic drug samples were used through the experiments, measuring of both positive and negative ICD peaks (Fig. 5B, Supplementary Fig. 1) suggests that the acridine moiety of the enantiomers adopts opposite chiral spatial arrangement in relation to the tryptophan indole ring.[17] Due to the different interaction energies of that binding modes, opposite CD activities are induced at slightly different wavelengths which do not completely cancel each other and result in the biphasic ICD spectrum (Fig. 5B, Supplementary Fig. 1). In addition, this mechanism explains loss of the vibrational fine structure of the UV and VIS absorption bands of AAG-bound QR (Fig. 5, Supplementary Fig. 1): absorption bands of the enantiomers are shifted in slightly different extents upon protein binding and their nearly complete overlap generates unstructured, bell-shaped peaks. Though no ICD bands were found with the 'F1/S' variant of AAG, the lack of ICD activity does not necessarily mean the lack of ligand–protein interactions. QR binds also to the 'F1/S' variant as suggested by alterations of its UV absorption (Supplementary Fig. 2) and fluorescence emission spectra (Fig. 9). In comparison with the 'A' variant, the 'CD-silent' binding site of the 'F1/S' variant is less hydrophobic (Fig. 9). The HSA binding of QR is very weak (Table 3).

Optical properties of MFQ prevented the direct ICD study of its protein binding. CD (Fig. 6) and fluorescence (Fig. 7) displacement experiments, however, demonstrated strong MFQ–AAG interaction (Table 2). CD displacement curves indicate that MFQ and AMQ share a common binding site, while partial displacement of PRQ and TFQ suggests adjacent, partly overlapping binding rooms for these drugs within the large cavity of AAG.[24]

Human pharmacokinetics of MFQ has been reported to be stereoselective, with higher plasma concentration for the (−)-enantiomer.[54,32] We found that the 'F1/S' genetic variant of AAG is responsible for the favored plasma protein binding of the (−)-isomer. To our knowledge, the inverse stereoselective binding of MFQ enantiomers to the AAG variants demonstrated here (Fig. 10) is the first example for this kind of racemic drug–AAG binding interaction. Though the binding of MFQ to HSA is weaker by about an order of magnitude, probably its contribution dominates in its extensive plasma binding.[33,34] Fluorescence displacement tests indicated that site I and site II are not involved in the MFQ–HSA interaction.

4. Implications of the results

1. Plasma protein binding of drugs might be important in practical sense when the degree of the binding exceeds 90%. Among the quinoline type antimalarial drugs investigated here, excessive plasma protein binding (>90%) of MFQ,[33,34] and PRQ[35] has been reported earlier. Our results pointed out that AAG is the most likely candidate being responsible for the high plasma protein binding of MFQ, PRQ, and QR. Due to its relatively low serum concentration (20–30 μM), AAG is a low-capacity drug carrier, thus variations of its plasma level might significantly alter unbound fractions of these high-affinity AAG ligand antimalarial agents. In addition, the 'F1/S' or 'A' variant selective binding of the antimalarial drugs (Table 1) further limits the binding capacity of AAG. Thus, free drug levels can be more influenced by the increase of the plasma AAG concentration observed in *Plasmodium* infections[13,15] and autoimmune diseases.[9] It is to be noted that the relative concentration of the AAG genetic variants also changes in acute-phase conditions[36,37] which can further modify the plasma distribution of antimalarial drugs showing variant binding preference (QR, PRQ, MFQ). Taking into account the similar HSA and AAG binding affinities of TFQ, plasma protein binding of this drug is principally determined by HSA present in large excess in blood.
2. To prevent the emergence and overcome drug-resistant malaria, artemisinin compounds are increasingly used in combination with older agents such as MFQ and AMQ.[38] Since the role of AAG in the plasma protein binding of artemisinins has been pointed out,[34,39,40] competitive plasma AAG binding interaction between these drugs can be considered. Among antibiotics[41,42] used to treat malaria in combination with classical antimalarial agents, lincomycin, clindamycin and erythromycin are the high-affinity ligands of AAG[2,9] which raises the possibility of antibiotic-antimalarial drug–drug competition for AAG binding sites. Similarly, high-affinity AAG drug ligands used in the supportive therapy of malaria patients like β-receptor blockers (e.g., propranolol), Ca^{2+} antagonists (e.g., verapamil), neuroleptics (e.g., chlorpromazine)[2,4] might compete for AAG binding sites with co-administered antimalarial drugs (QR, MFQ, PRQ).
3. When chiral drugs are administered in racemic form, the individual stereoisomers may bind to plasma proteins with different affinities, resulting in different free fractions. This effect might be practically significant, especially when the pharmacodynamic and/or the toxicology profiles of the enantiomers differ from each other. MFQ, PRQ, TFQ, and QR are all chiral drugs and used as racemates. Different in vivo antimalarial activity of QR, MFQ, and CLQ has been reported and ascribed mainly to the stereoselective differences in their pharmacokinetics.[43–45] Similarly to quinine and quinidine,[46] the (+)-isomer of MFQ was 1.7 times more active than the (−)-isomer against *P. falciparum* in vitro,[47] while the (−)-enantiomer is more potent in the adverse effect in the central nervous system.[43] Human pharmacokinetics of MFQ has been reported to be stereoselective, with higher plasma concentration for the (−)-enantiomer.[54,32] We found that the 'F1/S' genetic variant of AAG is responsible for the favored plasma protein binding

of the (−)-isomer. The opposite preferences detected in the binding of MFQ enantiomers to the genetic variants may result in interindividual differences.

4. Extrinsic CD activity of QR–AAG complexes is associated entirely to the 'A' variant. Thus, QR can be used as a novel selective CD marker suitable to study the 'A' variant selective binding of compounds which do not interfere with the ICD bands of QR between 250 and 300 nm.

5. Materials and methods

5.1. Materials

AMQ dihydrochloride (Sigma), (±)-CLQ diphosphate (Sigma), MFQ hydrochloride (Sigma, racemic mixture of the (−)-(11*S*,2′*R*)- and (+)-(11*R*,2′*S*)-*erythro* enantiomers), (±)-PRQ diphosphate (Aldrich), (±)-QR dihydrochloride (Fluka), quinaldine red (Sigma), (±)-propranolol hydrochloride (Sigma), mifepristone (Sigma), and diazepam (Sigma) were used as supplied. Chlorpromazine hydrochloride was obtained from EGIS Pharmaceuticals Ltd (Budapest, Hungary). (±)-Lorazepam acetate was synthesized as described.[48] AAG (99%, purified from Cohn Fraction VI) and HSA (⩾96%, essentially fatty acid free) were purchased from Sigma and used without further purification. TFQ was the gift from GlaxoSmithKline (Greenford, Middlesex, United Kingdom). Ligand stock solutions were prepared in double distilled water (PRQ, CLQ, AMQ, QR, propranolol, chlorpromazine), HPLC grade ethanol (TFQ, MFQ, mifepristone), or in DMSO (quinaldine red).

5.2. Isolation of genetic variants of AAG

Commercial 'native' AAG (Sigma) samples were subjected for separation of the two main genetic variants. The 'F1/S' and 'A' forms were separated as described previously.[49]

5.3. Preparation of AAG and HSA sample solutions

Protein samples were dissolved in physiological Ringer buffer solution (pH 7.4, 137 mM NaCl, 2.7 mM KCl, 0.8 mM $CaCl_2$, 1.1 mM $MgCl_2$, 1.5 mM KH_2PO_4 and 8.1 mM $Na_2HPO_4{\cdot}12H_2O$). Molar concentrations of AAG and HSA were determined spectrophotometrically: $\varepsilon_{278\,nm} = 33{,}500\ M^{-1}\,cm^{-1}$ for AAG[50] and $\varepsilon_{279\,nm} = 35{,}000\ M^{-1}\,cm^{-1}$ for HSA.[51]

5.4. Circular dichroism and UV/VIS absorption spectroscopy measurements

CD and UV/VIS spectra were recorded on a Jasco J-715 spectropolarimeter at 37 ± 0.2 °C under a constant nitrogen flow. Temperature control was provided by a Peltier thermostat equipped with magnetic stirring. For recording CD spectra, rectangular quartz cells of 1 cm optical pathlength (Hellma, USA) were used. All measurements were made in physiological Ringer buffer solution. Each spectrum represents the average of three scans (scan speed was 100 nm/min). UV/VIS absorption spectra were obtained by conversion of the high voltage (HT) values of the photomultiplier tube of the CD equipment into absorbance units. CD and absorption curves of drug-protein mixtures were corrected by subtracting the spectra of drug-free protein solutions.

JASCO CD spectropolarimeters record CD data as ellipticity ('Θ') in units of millidegrees (mdeg). The quantity of 'Θ' is converted to '$\Delta\varepsilon$' values using the equation $\Delta\varepsilon = \Theta/(33982cl)$, where '$\Delta\varepsilon$' is the molar circular dichroic absorption coefficient expressed in $M^{-1}\,cm^{-1}$, 'c' is the total drug concentration of the sample solutions (mol/L), and 'l' is the optical pathlength expressed in cm.[52]

5.5. Calculation of the binding parameters of drug–plasma protein complexes from ICD data

Details of the estimation of the association constants (K_a) and the number of binding sites (n) using ICD data have been described earlier.[51] Nonlinear regression analysis of the ICD values measured at different [drug]/[protein] molar ratios at fixed wavelength was performed by the NLREG® software (statistical analysis program, version 6.3 created by Philip H. Sherrod).

5.6. Fluorescence spectroscopy

Fluorescence measurements were carried out in a Shimadzu RF-1501 spectrofluorophotometer at room temperature (23 ± 1 °C), using quartz cuvette with 1 cm optical pathlength, both bandwidths were 10 nm. Aliquots of 2 mL AAG solutions (0.1 or 0.4 mg/mL) were measured alone, as well as in the presence of labels and displacers. Fluorescence intensities were corrected for the background. The quenching of bound quinaldine red fluorescence due to the ethanol content of additive stock solutions was also taken into consideration.

5.7. Chiral HPLC analysis of MFQ in ultrafiltrates

Ultrafiltrations were performed in the Amicon MPS-1 system, using YMT30 membranes at room temperature. The enantiomeric composition of free MFQ in the ultrafiltrates was determined by chiral HPLC method. The HPLC experiments were performed with a system composed of a Jasco PU-980 pump, a Rheodyne 7125 injector (20 μL loop), a Jasco MD 2010-Plus UV/VIS photodiode-array detector and Chrom Pass chromatographic software. Chiral-AAG column (100 × 4 mm i.d.) was obtained from ChromTech AB (Norsborg, Sweden). The mobile phase was 0.01 M phosphate buffer pH 5.3 containing 25% (v/v) acetonitrile, flow rate was 0.9 mL/min. The elution order, that is, first eluted (−)-(11*S*,2′*R*)- followed by (+)-(11*R*,2′*S*)-enantiomer of *erythro*-MFQ, was taken from Refs. 53 and 54.

5.8. HSA binding test

Chromatographic experiments on HSA-Sepharose gel were performed as described previously.[48] HSA (fatty acid free, Sigma) in 1% concentration was immobilized

on CNBr-activated Sepharose 4B (Pharmacia) and about 6 mL gel was filled into a glass column. Elution was made by Ringer buffer at room temperature, the flow rate was 1 mL/min. Ligand samples (5–20 μl of 0.5 mg/mL ethanolic or aqueous stock solutions) were applied manually. Elution volumes were determined by UV detection. Control experiments were performed on a gel containing no HSA. Only TFQ showed some retention due to non-specific adsorption, which was taken into consideration.

Acknowledgments

We thank GlaxoSmithKline for the gift of tafenoquine. This work was supported by research Grants of OTKA K69213, OTKA T049721, and NKFP 1/A/005/04 (MediChem 2 project). Skillful technical assistance by Ilona Kawka is appreciated.

Supplementary data

Supplementary data associated with this article can be found, in the online version, at doi:10.1016/j.bmc.2008.01.053.

References and notes

1. Ghuman, J.; Zunszain, P. A.; Petitpas, I.; Bhattacharya, A. A.; Otagiri, M.; Curry, S. *J. Mol. Biol.* **2005**, *353*, 38–52.
2. Israili, Z. H.; Dayton, P. G. *Drug Metab. Rev.* **2001**, *33*, 161–235.
3. Breustedt, D. A.; Schonfeld, D. L.; Skerra, A. *Biochim. Biophys. Acta* **2006**, *1764*, 161–173.
4. Herve, F.; Caron, G.; Duche, J. C.; Gaillard, P.; Abd Rahman, N.; Tsantili-Kakoulidou, A.; Carrupt, P. A.; d'Athis, P.; Tillement, J. P.; Testa, B. *Mol. Pharmacol.* **1998**, *54*, 129–138.
5. Fitos, I.; Visy, J.; Zsila, F.; Bikadi, Z.; Mady, G.; Simonyi, M. *Biochem. Pharmacol.* **2004**, *67*, 679–688.
6. Tomei, L.; Eap, C. B.; Baumann, P.; Dente, L. *Hum. Genet.* **1989**, *84*, 89–91.
7. Hochepied, T.; Berger, F. G.; Baumann, H.; Libert, C. *Cytokine Growth Factor Rev.* **2003**, *14*, 25–34.
8. Ritchie, R. F.; Palomaki, G. E.; Neveux, L. M.; Navolotskaia, O.; Ledue, T. B.; Craig, W. Y. *J. Clin. Lab. Anal.* **1999**, *13*, 273–279.
9. Kremer, J. M.; Wilting, J.; Janssen, L. H. *Pharmacol. Rev.* **1988**, *40*, 1–47.
10. Vangapandu, S.; Jain, M.; Kaur, K.; Patil, P.; Patel, S. R.; Jain, R. *Med. Res. Rev.* **2007**, *27*, 65–107.
11. Wallace, D. J. *Semin. Arthritis. Rheum.* **1989**, *18*, 282–296.
12. Borden, M. B.; Parke, A. L. *Drug Saf.* **2001**, *24*, 1055–1063.
13. Graninger, W.; Thalhammer, F.; Hollenstein, U.; Zotter, G. M.; Kremsner, P. G. *Acta Trop.* **1992**, *52*, 121–128.
14. Jagadeesan, V.; Krishnaswamy, K. *Eur. J. Clin. Pharmacol.* **1985**, *27*, 657–659.
15. Mansor, S. M.; Molyneux, M. E.; Taylor, T. E.; Ward, S. A.; Wirima, J. J.; Edwards, G. *Br. J. Clin. Pharmacol.* **1991**, *32*, 317–321.
16. Wanwimolruk, S.; Denton, J. R. *J. Pharm. Pharmacol.* **1992**, *44*, 806–811.
17. Zsila, F.; Iwao, Y. *Biochim. Biophys. Acta* **2007**, *1770*, 797–809.
18. Zsila, F.; Matsunaga, H.; Bikadi, Z.; Haginaka, J. *Biochim. Biophys. Acta* **2006**, *1760*, 1248–1273.
19. Zsila, F.; Bikádi, Z.; Fitos, I.; Simonyi, M. *Curr. Drug Discov. Technol.* **2004**, *1*, 133–153.
20. Ascoli, G. A.; Domenici, E.; Bertucci, C. *Chirality* **2006**, *18*, 667–679.
21. Maruyama, T.; Otagiri, M.; Takadate, A. *Chem. Pharm. Bull. (Tokyo)* **1990**, *38*, 1688–1691.
22. Nishi, K.; Fukunaga, N.; Otagiri, M. *Drug Metab. Dispos.* **2004**, *32*, 1069–1074.
23. Hazai, E.; Visy, J.; Fitos, I.; Bikadi, Z.; Simonyi, M. *Bioorg. Med. Chem.* **2006**, *14*, 1959–1965.
24. Albani, J. R. *Carbohydr. Res.* **2004**, *339*, 607–612.
25. Herve, F.; Gomas, E.; Duche, J. C.; Tillement, J. P. *Br. J. Clin. Pharmacol.* **1993**, *36*, 241–249.
26. Sudlow, G.; Birkett, D. J.; Wade, D. N. *Mol. Pharmacol.* **1976**, *12*, 1052–1061.
27. Fitos, I.; Visy, J.; Simonyi, M.; Hermansson, J. *Chirality* **1993**, *5*, 346–349.
28. Albani, J. R. *Carbohydr. Res.* **2006**, *341*, 2557–2564.
29. Ross, P. D.; Subramanian, S. *Biochemistry* **1981**, *20*, 3096–3102.
30. Lakowicz, J. R. In *Principles of Fluorescence Spectroscopy*; Springer, 2006; pp 185–210.
31. Ducharme, J.; Farinotti, R. *Clin. Pharmacokinet.* **1996**, *31*, 257–274.
32. Gimenez, F.; Pennie, R. A.; Koren, G.; Crevoisier, C.; Wainer, I. W.; Farinotti, R. *J. Pharm. Sci.* **1994**, *83*, 824–827.
33. Mu, J. Y.; Israili, Z. H.; Dayton, P. G. *Drug Metab. Dispos.* **1975**, *3*, 198–210.
34. Giao, P. T.; de Vries, P. J. *Clin. Pharmacokinet.* **2001**, *40*, 343–373.
35. Kennedy, E.; Frischer, H. *J. Lab. Clin. Med.* **1990**, *116*, 871–878.
36. Duche, J. C.; Urien, S.; Simon, N.; Malaurie, E.; Monnet, I.; Barre, J. *Clin. Biochem.* **2000**, *33*, 197–202.
37. Eap, C. B.; Fischer, J. F.; Baumann, P. *Clin. Chim. Acta* **1991**, *203*, 379–385.
38. Olliaro, P. L.; Taylor, W. R. *J. Postgrad. Med.* **2004**, *50*, 40–44.
39. Wanwimolruk, S.; Edwards, G.; Ward, S. A.; Breckenridge, A. M. *J. Pharm. Pharmacol.* **1992**, *44*, 940–942.
40. Colussi, D.; Parisot, C.; Legay, F.; Lefevre, G. *Eur. J. Pharm. Sci.* **1999**, *9*, 9–16.
41. Spizek, J.; Rezanka, T. *Appl. Microbiol. Biotechnol.* **2004**, *64*, 455–464.
42. Nakornchai, S.; Konthiang, P. *Acta Trop.* **2006**, *100*, 185–191.
43. Brocks, D. R.; Mehvar, R. *Clin. Pharmacokinet.* **2003**, *42*, 1359–1382.
44. Webster, R. V.; Craig, J. C.; Shyamala, V.; Kirby, G. C.; Warhurst, D. C. *Biochem. Pharmacol.* **1991**, *42*, S225–S227.
45. Bourahla, A.; Martin, C.; Gimenez, F.; Singhasivanon, V.; Attanath, P.; Sabchearon, A.; Chongsuphajaisiddhi, T.; Farinotti, R. *Eur. J. Clin. Pharmacol.* **1996**, *50*, 241–244.
46. Karle, J. M.; Karle, I. L. *Antimicrob. Agents Chemother.* **2002**, *46*, 1529–1534.
47. Karle, J. M.; Olmeda, R.; Gerena, L.; Milhous, W. K. *Exp. Parasitol.* **1993**, *76*, 345–351.
48. Fitos, I.; Tegyey, Z.; Simonyi, M.; Sjoholm, I.; Larsson, T.; Lagercrantz, C. *Biochem. Pharmacol.* **1986**, *35*, 263–269.
49. Fitos, I.; Visy, J.; Zsila, F.; Mády, G.; Simonyi, M. *Biochim. Biophys. Acta* **2006**, *1760*, 1704–1712.
50. Halsall, H. B.; Austin, R. C.; Dage, J. L.; Sun, H.; Schlueter, K. T. In *Proceedings of the International*

Symposium on Serum Albumin and α_1-Acid Glycoprotein: From Basic Sciences to Clinical Applications; Kumamoto, Japan, 2000; p. 45.
51. Zsila, F.; Bikádi, Z.; Simonyi, M. *Biochem. Pharmacol.* **2003**, *65*, 447–456.
52. Woody, R. W. *Methods Enzymol.* **1995**, *246*, 34–71.
53. Aubry, A. F.; Gimenez, F.; Farinotti, R.; Wainer, I. W. *Chirality* **1992**, *4*, 30–35.
54. Wallen, L.; Ericsson, O.; Wikstrom, I.; Hellgren, U. *J. Chromatogr. B Biomed. Appl.* **1994**, *655*, 153–157.